Heterometallic Network Complexes of the Ambidentate, Extended-Reach Linear Ligand 1-(4′-pyridyl)pyridin-4-one

David M. L. Goodgame,* David A. Grachvogel, Andrew J. P. White, and David J. Williams*

Department of Chemistry, Imperial College of Science, Technology and Medicine, London SW7 2AY, U.K.

Received June 4, 2001

An investigation into the ability of the ambidentate, "extended-reach" ligand 1-(4′-pyridyl)pyridin-4-one (pypyd) to form polymeric network complexes has resulted in the X-ray characterization of the compounds $[Cu(pypyd)_2(H_2O)_2](ClO_4)_2 \cdot pypyd$ **1**, $[Co_2Dy_2(pypyd)_8(H_2O)_2(NCS)_4(NO_3)_4][Co(NCS)_4]$ **2**, and $[NiYb(pypyd)_4(NCS)_2(NO_3)_2](NO_3)$ **3**. The homometallic copper complex, **1**, forms a (4,4) sheet polymer with additional intrasheet cross-linking via hydrogen bonding of noncoordinated pypyd molecules to the aqua ligands on the Cu centers. The heterometallic Co/Dy complex, **2**, also produces a contiguous (4,4) sheet but without the hydrogen bonded pypyd cross-link. The heterometallic Ni/Yb compound, **3**, forms a more complex array comprised of mutually interpenetrating networks each of three-dimensional (6,4) topology. The crystal structure of an acetic acid adduct of pypyd, **4**, is also reported.

Introduction

In the rapidly expanding field of coordination polymer chemistry, considerable use has been made of the rigid linear bridging ligand 4,4′-bipyridyl and also of related ligands in which pairs of 4-pyridyl units are connected by various "spacer" groups.[1−9] In contrast to the veritable plethora of reports concerning the network-forming ability of these and other types of what one might term *isodentate* ligands (i.e., those providing equivalent donor groups), those involving the use of similar, uncharged *ambidentate* ligands containing two different donor atoms are decidedly sparse[10−12] (polymers containing short anionic bridges such as CN^- and NCS^- are, of course, well-documented).

The use of ambidentate "extended reach" ligands is attractive not only because of the potential for generating new types of network structures but also for the opportunity it offers for forming heterometallic complexes involving various combinations of metal ion node points. Such combinations could, in principle, lead to the formation of materials with interesting and useful properties deriving from the presence of the heterometallic arrays (e.g., magnetic cooperativity, electron-transfer processes, etc.).

As our starting point to explore this field, we have investigated the efficacy of the ligand 1-(4′-pyridyl)pyridin-4-one (pypyd).[13] To illustrate some of the types of network product that can be obtained with this ligand, we report here the results of structural studies on one homometallic (Cu^{II}) and two heterometallic (Co^{II}/Dy^{III} and Ni^{II}/Yb^{III}) complexes. We describe also the structure of an acetic acid adduct of pypyd.

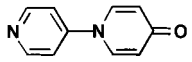

pypyd

Experimental Section

Preparation of Compounds. The ligand 1-(4′-pyridyl)pyridin-4-one was prepared by the literature method[13] but with recrystallization of the crude brown product from toluene rather than benzene and employing decolorising charcoal during recrystallization.

Metal Complexes. *$[Cu(pypd)_2(H_2O)_2](ClO_4)_2 \cdot pypyd$ (**1**) and $[Cu(pypyd)_2(H_2O)_2](ClO_4)_2$.* **CAUTION!** *Although we did not observe any explosive behavior with either of the perchlorate compounds described below, all metal perchlorates must be regarded as potentially explosive and appropriate safety measures must be taken (see, for example, J. Chem. Educ. **1973**, 50, A335).* Blue-green prisms of **1** suitable for X-ray analysis were obtained from a solution of copper(II) perchlorate hexahydrate (0.1 mmol) and pypyd (0.2 mmol) in a mixture of methanol (2 mL) and acetone (4 mL). After crystal selection, the bulk sample was collected, washed with diethyl ether, and dried in vacuo to give a green product analyzing as $[Cu(pypyd)_2(H_2O)_2](ClO_4)_2$. Anal. Calcd for $C_{20}H_{20}Cl_2CuN_4O_{12}$: C, 37.4; H, 3.1; N, 8.7. Found: C, 38.0; H, 2.9; N, 9.0. EPR (X-band) $g_{eff} = 2.071, 2.258$. IR (CsI, cm^{-1}): 1641 ν(CO), 1095 $\nu_3(ClO_4^-)$, 624 $\nu_4(ClO_4^-)$.

*$[Co_2Dy_2(pypyd)_8(H_2O)_2(NCS)_4(NO_3)_4][Co(NCS)_4]$ (**2**).* Blue rhombic crystals of **2** suitable for X-ray analysis were grown by mixing solutions of cobalt(II) thiocyanate (0.1 mmol), dysprosium nitrate hexahydrate (0.1 mmol), and pypyd (0.4 mmol) in a 1:1 mixture of acetone and methanol (10 mL) and storing the resulting solution in a desiccator

(1) Stang, P. J.; Olenyuk, B. *Acc. Chem. Res*. **1997**, *30*, 502.
(2) Batten, S. R.; Robson, R. *Angew. Chem., Int. Ed.* **1998**, *37*, 1460 and references therein.
(3) Kitagawa, S.; Kondo, M. *Bull. Chem. Soc. Jpn.* **1998**, *71*, 1739 and references therein.
(4) Blake, A. J.; Champness, N. R.; Hubberstey, P.; Li, W. S.; Withersby, M. A.; Schroder, M. *Coord. Chem. Rev.* **1999**, *183*, 117.
(5) Fujita, M. *Chem. Soc. Rev.* **1998**, *27*, 417.
(6) Leininger, S.; Olenyuk, B.; Stang, P. J. *Chem. Rev.* **2000**, *100*, 853.
(7) Zaworotko, M. J. *Angew. Chem., Int. Ed.* **2000**, *39*, 3052 and references therein.
(8) Swiegers, G. F.; Malefetse, T. J. *Chem. Rev.* **2000**, *100*, 3483.
(9) Robson, R. *J. Chem. Soc., Dalton Trans.* **2000**, 3735 and references therein.
(10) Goodgame, D. M. L.; Menzer, S.; Ross, A. T.; Williams, D. J. *J. Chem. Soc., Chem. Commun.* **1994**, 2605.
(11) Duncan, P. C. M.; Goodgame, D. M. L.; Hitchman, M. A.; Menzer, S.; Stratemeier, H.; Williams, D. J. *J. Chem. Soc., Chem. Commun.* **1994**, 2605.
(12) Hong, M.; Su, W.; Cao, R.; Fujita, M.; Lu, J. *Chem. Eur. J.* **2000**, *6*, 427.
(13) Arndt, F. *Chem. Ber.* **1932**, *65*, 92.

10.1021/ic010590h CCC: $20.00
Published on Web 10/02/2001

Table 1. Crystallographic Data for Compounds **1**−**4**

data	**1**	**2**	**3**	**4**
chem formula	$[C_{20}H_{20}CuN_4O_4](ClO_4)_2\cdot C_{10}H_8N_2O$	$[C_{84}H_{68}N_{24}O_{22}S_4Co_2Dy_2]\cdot[(SCN)_4Co]\cdot 3MeOH\cdot 4H_2O$	$[C_{42}H_{32}N_{12}O_{10}S_2NiYb](NO_3)\cdot 3.5MeOH\cdot 2H_2O$	$C_{10}H_8N_2O\cdot CH_3CO_2H$
fw	815.0	2796.2	1370.9	232.2
space group	$P2_1/c$ (No. 14)	$C2$ (No. 5)	$P2_1/n$ (No. 14)	$P2_1/c$ (No. 14)
T (°C)	20	−70	−70	−70
a, Å	6.380(1)	34.565(7)	15.169(4)	3.806(1)
b, Å	19.874(2)	17.060(2)	19.067(2)	10.448(2)
c, Å	12.916(1)	12.646(2)	24.303(3)	28.290(7)
β, deg	101.03(1)	99.88(2)	92.66(1)	90.58(2)
V, Å^3	1607.5(2)	7347(2)	7022(2)	1124.9(4)
Z	2[a]	2[b]	4	4
ρ_{calcd}, g cm^{-3}	1.684	1.264	1.297	1.371
λ, Å	1.54178	0.71073	0.71073	1.54178
μ, mm^{-1}	3.19	1.52	1.72	0.83
independent data	2392	6715	9176	1695
observed data[c]	2093	5171	5428	1254
parameters	331	740	977	159
R_1[d]	0.042	0.063	0.077	0.055
wR_2[e]	0.108	0.148	0.178	0.135

[a] The complex has crystallographic C_i symmetry. [b] The complex has crystallographic C_2 symmetry. [c] $|F_o| > 4\sigma(|F_o|)$. [d] $R_1 = \sum||F_o| - |F_c||/\sum|F_o|$. [e] $wR_2 = \{\sum[w(F_o^2 - F_c^2)^2]/\sum[w(F_o^2)^2]\}^{1/2}$; $w^{-1} = \sigma^2(F_o^2) + (aP)^2 + bP$.

over concentrated H_2SO_4 for 3 days. After crystal selection the bulk sample was collected and dried in vacuo to give a blue product analyzing as $Co_3Dy_2(pypyd)_8(NCS)_8(NO_3)_4(H_2O)_6$. Yield: 36%. Anal. Calcd for $C_{88}H_{72}Co_3Dy_2N_{28}O_{24}S_8$: C, 39.2; H, 2.8; N, 14.5. Found: C, 39.6; H, 2.7; N, 14.4. IR (CsI, cm^{-1}): 2070 br ν(NCS), 1638 ν(CO).

*[NiYb(pypyd)$_4$(NCS)$_2$(NO$_3$)$_2$](NO$_3$) (**3**).* Crystals suitable for X-ray characterization were obtained by addition of a solution of pypyd (0.4 mmol) in 8 mL of a 1:1 mixture of acetone and methanol to a solution of nickel(II) thiocyanate (0.1 mmol) and hydrated ytterbium(III) nitrate (0.1 mmol) in methanol (2.6 mL) followed by storage in a desiccator over concentrated H_2SO_4 for 3 days. After crystal selection the bulk sample was collected, and dried to give a pale purple product (76% yield) analyzing as $NiYb(pypyd)_4(NCS)_2(NO_3)_3(H_2O)_2$. Anal. Calcd for $C_{42}H_{36}N_{13}NiO_{15}S_2Yb$: C, 40.1; H, 2.9; N, 14.5. Found: C, 40.0; H, 3.0; N, 14.7. IR (CsI, cm^{-1}): 2086 ν(NCS), 1640 ν(CO).

*(pypyd)·CH$_3$CO$_2$H (**4**).* This was obtained as fine, hair-like needles suitable for X-ray study by recrystallizing the brown crude product of the original reaction mixture from acetonitrile instead of toluene.

Microanalyses and Spectroscopic Measurements. Elemental analyses were performed by the Scientific Analysis and Consultancy Service, University of North London, and the spectroscopic measurements were made as described previously.[14]

Crystallographic Analyses. Table 1 provides a summary of the crystallographic data for compounds **1**−**4**. In each case, data were collected on Siemens P4/PC diffractometers using ω-scans. The structures of **1** and **4** were solved by direct methods, and those of **2** and **3** were solved by the heavy atom method, and they were all refined based on F^2 using the SHELXTL program system.[15] The polarity of **2** was determined by a combination of R-factor tests [$R_1^+ = 0.0633$ and $R_1^- = 0.0652$] and by use of the Flack parameter [$x^+ = +0.20(5)$ and $x^- = +0.80(5)$]. The structure of **3** exhibits significant disorder in the ytterbium coordination sphere, with two partial occupancy orientations being identified for each of the pyridone rings of the four pypyd ring systems and also for the two coordinated nitrate ligands. In each case, only the major occupancy non-hydrogen atoms were refined anisotropically. CCDC 171300 − 171303. Selected bond lengths and angles are given in Tables 2−5.

Results and Discussion

Structure of [Cu(pypyd)$_2$(H$_2$O)$_2$](ClO$_4$)$_2$·pypyd (1). The X-ray analysis of the crystals of complex **1** showed it to contain two unique pypyd molecules, one of which coordinates via both its pyridone oxygen atom and its pyridyl nitrogen atom to copper centers, whereas the other is involved only in hydrogen bonded linkages. The geometry at each copper center is centrosymmetric and is severely tetragonally distorted octahedral, with the copper atom being bonded to the pyridone oxygen atoms of two pypyd ligands and to the pyridyl nitrogen atoms of another pair. The axial sites at copper are occupied by aqua ligands (Figure 1). The pattern of bonding at copper is unexceptional, with Cu−N(py) = 2.017(3), Cu−O(pyd) = 1.977(2) Å, and with long Cu−O(aqua) = 2.490(4) Å; the cis angles at Cu range from 86.6(1) to 93.5(1)°.

Table 2. Selected Bond Lengths (Å) and Angles (deg) for **1**

Cu−N(1A)	2.017(3)	Cu−O(13)	1.977(2)
Cu−O(40)	2.490(4)		
O(13)−Cu−N(1B)	92.89(10)	O(13)−Cu−N(1A)	87.11(10)
O(13)−Cu−O(40C)	93.45(12)	N(1A)−Cu−O(40C)	87.39(14)
O(13)−Cu−O(40)	86.55(12)	N(1A)−Cu−O(40)	92.61(14)

Both the coordinated and the noncoordinated pypyd units are nonplanar, having torsional twists about their central linking bonds of ca. 22 and 20°, respectively.

The bridging, ambidentate role of the coordinated pypyd ligand gives rise to the formation of a (4,4) sheet comprising contiguous diamond-shaped rings (Figure 2) with *trans*-annular Cu···Cu separations of 12.92 and 19.87 Å. The shorter diagonals within the net are bridged by the noncoordinated pypyd molecules by virtue of hydrogen bonds from the axial aqua ligands to the terminal N and O atoms, respectively. The O−H···O hydrogen bonds are short [O···O 2.56 Å, H···O 1.67 Å, and O−H···O 169°], whereas their O−H···N counterparts to the pyridyl nitrogen atom are much longer [O···N 3.09 Å, H···N 2.23 Å, and O−H···N 160°]. It should be noted, however, that the central C(18)−N(21) bond of the noncoordinated pypyd molecule is positioned over a crystallographic inversion center, and therefore, there is a statistical reversal of the N(15)−O(27) axis throughout the structure. This "reversal" however does not change the cross-linking hydrogen bonding role of this unit.

Adjacent sheets are aligned in register with respect to the crystallographic *a* axis. The shortest intersheet contact is between the aqua hydrogen atom (not involved in intrasheet hydrogen bonding) in one sheet and the aqua oxygen atom in the next; the H···O distance is 2.41 Å, which is rather long for

(14) Atherton, Z.; Goodgame, D. M. L.; Menzer, S.; Williams, D. J. *Inorg. Chem.* **1998**, *37*, 849.
(15) *SHELXTL PC*, version 5.03; Siemens Analytical X-ray Instruments Inc.: Madison, WI, 1994.

Table 3. Selected Bond Lengths (Å) and Angles (deg) for **2**

Dy−O(10)	2.395(9)	Dy−O(22)	2.337(8)
Dy−O(34)	2.324(11)	Dy−O(46)	2.327(9)
Dy−O(57)	2.607(13)	Dy−O(58)	2.47(2)
Dy−O(61)	2.524(14)	Dy−O(62)	2.629(12)
Dy−O(64)	2.470(14)	Co(1)−N(1)	2.19(2)
Co(1)−N(13A)	2.17(2)	Co(1)−N(50)	2.04(2)
Co(2)−N(25)	2.18(2)	Co(2)−N(37A)	2.16(2)
Co(2)−N(53)	2.006(13)	Co(3)−N(70)	1.95(2)
Co(3)−N(73)	1.94(3)		
O(34)−Dy−O(46)	86.3(4)	O(34)−Dy−O(22)	85.6(4)
O(46)−Dy−O(22)	154.4(4)	O(34)−Dy−O(10)	142.6(5)
O(46)−Dy−O(10)	85.5(3)	O(22)−Dy−O(10)	86.2(3)
O(34)−Dy−O(64)	71.5(4)	O(46)−Dy−O(64)	77.7(5)
O(22)−Dy−O(64)	76.7(5)	O(10)−Dy−O(64)	71.1(5)
O(34)−Dy−O(58)	139.1(4)	O(46)−Dy−O(58)	123.2(4)
O(22)−Dy−O(58)	77.1(4)	O(10)−Dy−O(58)	73.4(5)
O(64)−Dy−O(58)	136.7(5)	O(34)−Dy−O(61)	76.6(5)
O(46)−Dy−O(61)	79.8(5)	O(22)−Dy−O(61)	121.6(5)
O(10)−Dy−O(61)	137.2(5)	O(64)−Dy−O(61)	141.7(5)
O(58)−Dy−O(61)	81.5(6)	O(34)−Dy−O(57)	141.2(4)
O(46)−Dy−O(57)	73.4(4)	O(22)−Dy−O(57)	125.6(4)
O(10)−Dy−O(57)	69.6(4)	O(64)−Dy−O(57)	132.4(5)
O(58)−Dy−O(57)	49.9(4)	O(61)−Dy−O(57)	67.6(5)
O(34)−Dy−O(62)	70.2(5)	O(46)−Dy−O(62)	126.3(4)
O(22)−Dy−O(62)	73.1(4)	O(10)−Dy−O(62)	140.5(4)
O(64)−Dy−O(62)	132.3(5)	O(58)−Dy−O(62)	69.4(5)
O(61)−Dy−O(62)	48.5(5)	O(57)−Dy−O(62)	95.3(5)
N(50A)−Co(1)−N(50)	178.3(14)	N(50)−Co(1)−N(13A)	92.9(8)
N(50)−Co(1)−N(13B)	88.3(8)	N(13A)−Co(1)−N(13B)	93.2(9)
N(50)−Co(1)−N(1)	91.9(7)	N(13A)−Co(1)−N(1)	175.2(9)
N(50)−Co(1)−N(1A)	86.9(7)	N(13A)−Co(1)−N(1A)	87.7(4)
N(1)−Co(1)−N(1A)	91.7(9)	N(53)−Co(2)−N(53A)	175.7(10)
N(53)−Co(2)−N(37B)	87.2(7)	N(53)−Co(2)−N(37A)	89.9(7)
N(37B)−Co(2)−N(37A)	95.7(10)	N(53)−Co(2)−N(25)	91.2(6)
N(37B)−Co(2)−N(25)	87.8(4)	N(37A)−Co(2)−N(25)	176.4(8)
N(53)−Co(2)−N(25A)	91.9(6)	N(25)−Co(2)−N(25A)	88.7(7)
N(73A)−Co(3)−N(73)	103.4(12)	N(73)−Co(3)−N(70A)	116.0(8)
N(73)−Co(3)−N(70)	105.2(9)	N(70A)−Co(3)−N(70)	111.1(10)

Table 4. Selected Bond Lengths (Å) and Angles (deg) for **3**

Yb−O(12)	2.22(2)	Yb−O(24A)	2.274(12)
Yb−O(36A)	2.19(2)	Yb−O(48A)	2.265(14)
Yb−O(58)	2.43(2)	Yb−O(59)	2.40(2)
Yb−O(62)	2.42(2)	Yb−O(63)	2.459(14)
Ni−N(1)	2.133(10)	Ni−N(13)	2.130(10)
Ni−N(25)	2.130(11)	Ni−N(37)	2.112(10)
Ni−N(50)	2.03(2)	Ni−N(53)	2.08(2)
O(36A)−Yb−O(12)	174.2(7)	O(36A)−Yb−O(48A)	94.2(6)
O(12)−Yb−O(48A)	91.6(6)	O(36A)−Yb−O(24A)	81.9(6)
O(12)−Yb−O(24A)	92.5(6)	O(48A)−Yb−O(24A)	171.4(6)
O(36A)−Yb−O(59)	103.1(7)	O(12)−Yb−O(59)	77.2(6)
O(48A)−Yb−O(59)	93.5(6)	O(24A)−Yb−O(59)	80.0(5)
O(36A)−Yb−O(62)	101.8(7)	O(12)−Yb−O(62)	80.1(6)
O(48A)−Yb−O(62)	63.7(6)	O(24A)−Yb−O(62)	124.5(5)
O(59)−Yb−O(62)	147.3(6)	O(36A)−Yb−O(58)	50.5(7)
O(12)−Yb−O(58)	130.2(6)	O(48A)−Yb−O(58)	91.1(7)
O(24A)−Yb−O(58)	80.5(6)	O(59)−Yb−O(58)	53.0(5)
O(62)−Yb−O(58)	142.9(6)	O(36A)−Yb−O(63)	101.0(7)
O(12)−Yb−O(63)	75.7(6)	O(48A)−Yb−O(63)	115.7(6)
O(24A)−Yb−O(63)	72.7(5)	O(59)−Yb−O(63)	140.3(5)
O(62)−Yb−O(63)	52.0(5)	O(58)−Yb−O(63)	143.8(5)
N(50)−Ni−N(53)	179.6(5)	N(50)−Ni−N(37)	90.8(5)
N(53)−Ni−N(37)	89.4(5)	N(50)−Ni−N(25)	89.5(5)
N(53)−Ni−N(25)	90.9(5)	N(37)−Ni−N(25)	91.1(4)
N(50)−Ni−N(13)	89.4(5)	N(53)−Ni−N(13)	90.5(5)
N(37)−Ni−N(13)	179.8(5)	N(25)−Ni−N(13)	88.8(4)
N(50)−Ni−N(1)	90.1(5)	N(53)−Ni−N(1)	89.6(5)
N(37)−Ni−N(1)	90.9(4)	N(25)−Ni−N(1)	177.9(4)
N(13)−Ni−N(1)	89.2(4)		

any significant hydrogen bonding. Similarly, the shortest intersheet $\pi-\pi$ separation is 3.97 Å. There is, however, an intramolecular $\pi-\pi$ stacking interaction between the coordinated pyridone ring and its hydrogen-bonded, noncoordinated counterpart; the centroid−centroid and mean interplanar separations are 4.19 and 3.67 Å, respectively, the rings being inclined by ca. 7°. The perchlorate counteranions are disordered and are located in voids formed between the sheets.

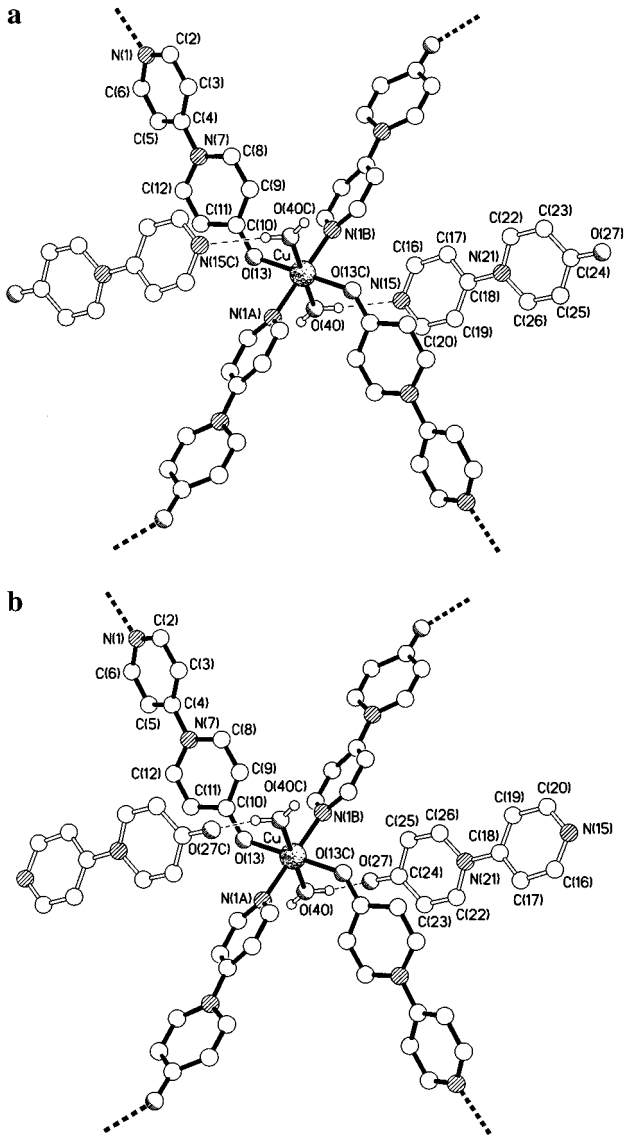

Figure 1. Coordination at copper in the structure of **1** showing the relative dispositions of the four coordinated pypyd ligands and the hydrogen bonding (a) to the pyridyl nitrogen atom of a pair of noncoordinated pypyd molecules and (b) to the oxygen atom of a pair of noncoordinated pypyd molecules.

Table 5. Selected Bond Lengths (Å) for **4**

N(1)−C(6)	1.331(5)	N(1)−C(2)	1.339(5)
C(2)−C(3)	1.390(4)	C(3)−C(4)	1.375(4)
C(4)−C(5)	1.394(4)	C(4)−N(7)	1.439(4)
C(5)−C(6)	1.381(5)	N(7)−C(12)	1.367(4)
N(7)−C(8)	1.369(3)	C(8)−C(9)	1.356(4)
C(9)−C(10)	1.435(4)	C(10)−O(10)	1.261(4)
C(10)−C(11)	1.432(4)	C(11)−C(12)	1.351(4)
C(20)−O(20)	1.207(4)	C(20)−O(21)	1.306(4)
C(20)−C(22)	1.496(5)		

Microanalysis results on a powdered sample of **1**, after thorough washing with diethyl ether, suggest that the cross-linking noncoordinated pypyd molecules are not firmly held as that product had the stoichiometry $[Cu(pypyd)_2(H_2O)_2](ClO_4)_2$.

Structure of $[Co_2Dy_2(pypyd)_8(H_2O)_2(NCS)_4(NO_3)_4][Co(NCS)_4]$ (2). Crystals of **2** were shown to have the composition $[Co_2Dy_2(pypyd)_8(H_2O)_2(NCS)_4(NO_3)_4][Co(NCS)_4]\cdot 3MeOH\cdot 4H_2O$ and a structure (Figure 3) in which the dysprosium atom

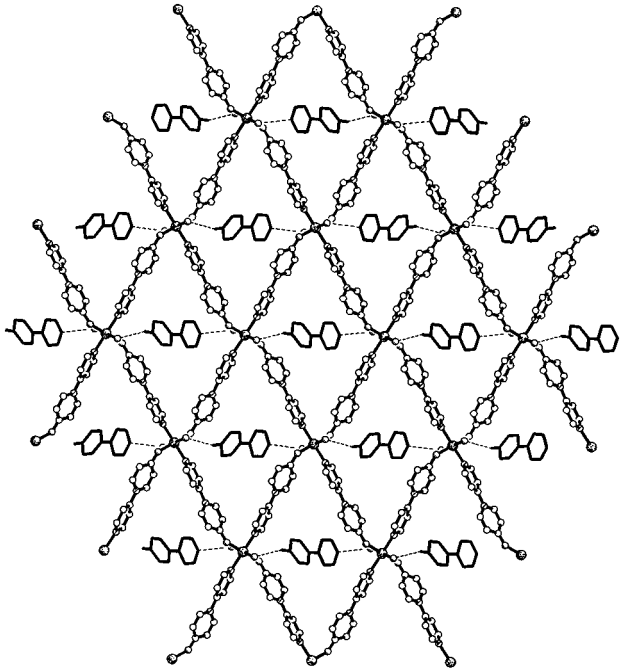

Figure 2. Part of the sheet network in the structure of **1** showing the cross-linking via hydrogen bonding of the short diagonal in each of the diamond-shaped macrocyclic rings.

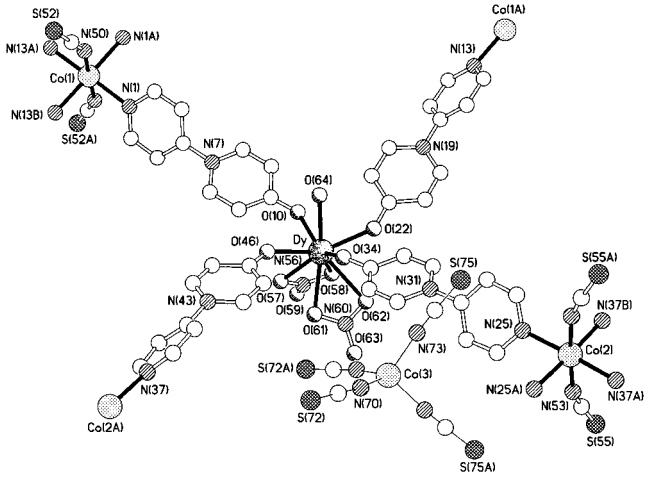

Figure 3. Principal structural unit in **2** showing the monocapped square antiprismatic and octahedral coordination geometries at Dy and Co, respectively, and their linking by pypyd bridges. The $Co(NCS)_4^{2-}$ anion is also depicted.

is coordinated to the oxygen atom of each of the four pypyd ligands, two nitrate groups, and an aqua ligand. The coordination geometry is a distorted monocapped square antiprism, with the aqua ligand occupying the capping position. The Dy···O distances fall into two distinct groups with those to the pypyd ligands being shorter than those to the remaining coordinated oxygen atoms (Table 3).

The four pypyd ligands have nonplanar conformations with torsional twists about their central C−N bonds of between 40 and 52°. The pyridyl nitrogen atom of each of these ligands bonds to a cobalt center. The structure contains three independent cobalt centers two of which are coordinated to the pypyd ligands, whereas the third forms the core of a $Co(NCS)_4^{2-}$ anion. The geometry at this latter cobalt center is distorted tetrahedral with N−Co−N angles in the range of 103.4 (12)−116.0 (8)°, whereas the other two have distorted octahedral coordination geometries, being bound to two trans-axial isothiocyanate

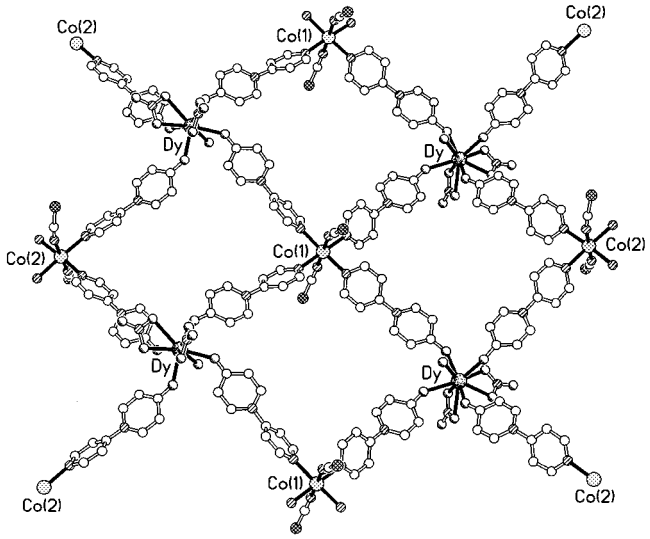

Figure 4. Contiguous (4,4) sheet in the structure of **2**.

ligands and four equatorial pypyd molecules. All three cobalt atoms lie on crystallographic C_2 axes.

The linking of the dysprosium and cobalt centers by the pypyd ligands produces a contiguous (4,4) sheet very similar to that seen in **1** but without the additional hydrogen bonded pypyd cross-link (Figure 4). Because of the two independent cobalt centers, there are three different macrocycles present within the grid: those with pairs of Co(1) at opposite corners, those with pairs of Co(2), and those with Co(1) and Co(2) combinations. The geometries of these three types of rings are very similar and, within the grid, the edge Dy···Co distances are 12.30 and 12.49 Å. The trans-annular Dy···Dy distances range between 17.06 and 18.22 Å, and the Co···Co lengths from 17.06 to 17.35 Å.

Each net has a slightly sinusoidal profile, and adjacent sheets are stacked offset with respect to each other in a face-to-face and back-to-back arrangement and have the nitrates attached to the dysprosium atoms in one sheet inserted into the "window" created by a $Dy_2Co(1)Co(2)$ macrocycle in the next. The $Co(NCS)_4^{2-}$ anions are located in the cavities created by the sinusoidal nature of adjacent sheets and the coincidence of the "peaks" of one sheet with the "troughs" of the next. A plan view of this arrangement is illustrated schematically in Figure 5, where the nitrate groups having been omitted for clarity. The included solvent molecules are distributed in secondary voids between the sheets.

Structure of $[NiYb(pypyd)_4(NCS)_2(NO_3)_2](NO_3)$ (3). Use of nickel thiocyanate in place of cobalt thiocyanate and replacement of dysprosium nitrate with ytterbium nitrate afforded crystals of a complex shown by X-ray analysis to have the composition $[NiYb(pypyd)_4(NCS)_2(NO_3)_2](NO_3)\cdot 3.5MeOH\cdot 2H_2O$. As with **2**, a heterometallic network was obtained, one which is only subtly different at the covalent level but substantially different at the supramolecular level. Each nickel center is again bonded to the nitrogen atoms of four pypyd ligands and two isothiocyanate groups in a slightly distorted octahedral geometry, with the anions in the trans positions (Figure 6). The lanthanide center is bonded to two chelating nitrate groups and four O-bonded pypyd ligands but, in this case, no aqua ligand. The geometry at Yb is distorted square antiprismatic, with the Yb−O(nitrate) distances all longer than those to the pyridone oxygen atoms (Table 4). This coordination geometry can also be visualized as distorted "octahedral" with the chelating nitrate groups as the "axial" ligands. It should be

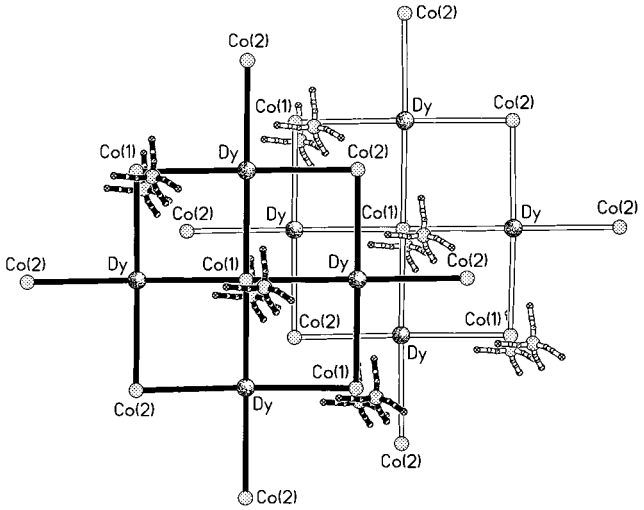

Figure 5. Schematic representation showing the relative dispositions of adjacent sheets in **2** and the siting of the $Co(NCS)_4^{2-}$ anions. The nitrates attached to each Dy center in one sheet which protrude through the "windows" in adjacent sheets have been omitted for clarity.

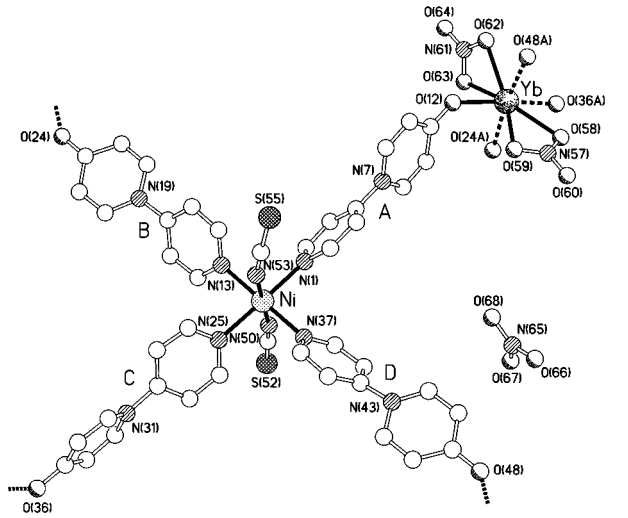

Figure 6. Principal structural unit in **3** showing the respective 8 and 6 coordination at Yb and Ni and their linking by pypyd bridges. One of the partial occupancy, noncoordinated nitrate anions is also shown. The four independent pypyd ligands are identified as A, B, C, and D.

noted that in this structure there is disorder which involves both alternate conformations of the bridging pypyd ligands and concomitant differences in the orientations of the coordinated nitrates. The figures illustrate the major occupancy conformers.

In the structure of **3**, both metals lie in general crystallographic positions, whereas in **2**, the cobalt atoms are positioned on C_2 axes of symmetry. All four crystallographically independent pypyd ligands (A−D in Figure 7) bridge directly adjacent nickel and ytterbium centers but, surprisingly, produce macrocycles of twice the size of those in **2**. In **3**, each macrocycle comprises three nickel atoms, three ytterbium atoms, and six pypyd ligands (cf. the 2:2:4 ratio in **2**). Two types of macrocycle are present, each with an approximately rectangular shape and with similar dimensions. One is comprised of pairs of A, B, and C type linking pypyd ligands whereas the other contains pairs of A, C, and D ligands. The shortest trans-annular Yb···Ni separations are 11.83 and 12.54 Å in the two independent macrocycles, respectively.

The principal difference in this structure compared to that of **2** is in the relative orientations of the nickel octahedron with

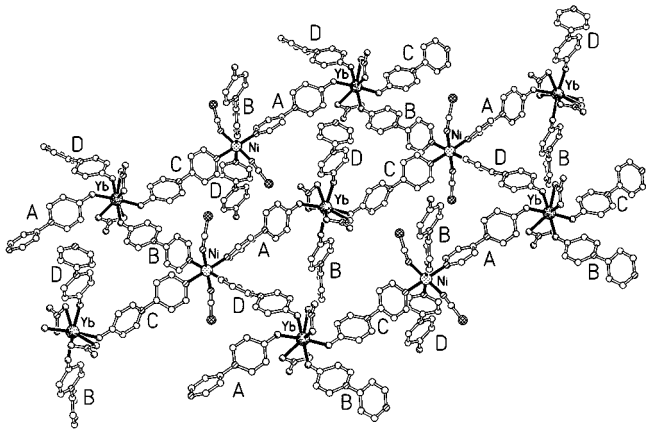

Figure 7. Part of the 3D net in the structure of **3** showing the two principal elongated macrocycles of type ABCABC and ACDACD. The pypyd ligands oriented orthogonally to the "sheet" that links this "sheet" to its neighbor are also illustrated.

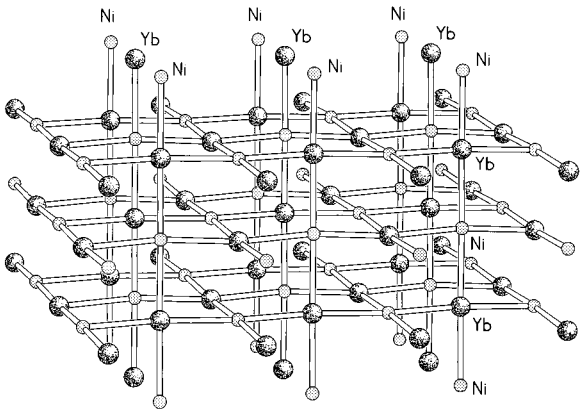

Figure 8. Schematic representation of the 3D net in **3** showing only the Ni and Yb centers.

respect to the ytterbium coordination polyhedron. In **3**, the SCN−Ni−NCS axis of the nickel octahedron is oriented approximately orthogonal to the ONO_2−Yb−O_2NO "axis" at the ytterbium center, whereas in **2** one of the Dy−O_2NO vectors is co-directional with one of the Co−NCS directions. As a consequence, whereas in **2** discrete sheets are formed, here in **3**, a 3D network is produced as illustrated schematically in Figure 8. This type of linkage, which was shown by Wells to be the simplest topological representation of the structures of the fibrous zeolites edingtonite, thomsonite, and natrolite,[16] closely resembles that seen in the homometallic 3D network formed by $[Co(HMBA)_3][Co(NCS)_4]$, where HMBA = hexamethylenebisacetamide.[17]

There are substantial pores in the polymeric structure of **3**, the edge lengths between the metals at the corners of the rectangular channels being ca. 10 and 20 Å, respectively. As frequently happens with such networks in the absence of large included ions or molecules, the networks mutually interpenetrate and are thus self-filling (Figure 9). The small residual voids within this matrix are occupied by the disordered, noncoordinated nitrate counteranions and trapped solvent molecules.

Structure of the Acetic Acid Adduct of 1-(4′-Pyridyl)-pyridin-4-one. We also attempted to obtain crystals of the free

(16) Wells. A. F. *Three-Dimensional Nets and Polyhedra*; Wiley-Interscience: New York, 1977; p 1259.
(17) Chatterton, N. P.; Goodgame, D. M. L.; Grachvogel, D. A.; Hussain, I.; White, A. J. P.; Williams, D. J. *Inorg. Chem.* **2001**, *40*, 312.

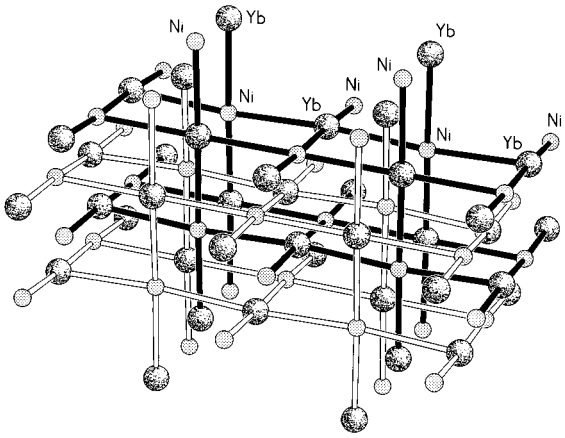

Figure 9. Schematic representation of the mutual interpenetration of the 3D nets in **3**. Only the Ni and Yb centers are shown.

pypyd ligand for X-ray characterization and, thereby, for comparison with its behavior toward metal ions and its efficacy as a bridging unit. Unfortunately, despite exploring the use of a wide range of recyrstallisation solvents (some twenty in all), we were only able to obtain X-ray quality crystals, as fine hair-like needles, of the 1:1 acetic acid adduct, pypyd·CH_3CO_2H, **4**, derived from the acetic acid produced during the reaction between the pyridin-4-one and the acetic anhydride.

The structure of **4** (Figure 10) shows the pypyd molecule to have a quinone-like pattern of bonding within the pyridone moiety, the C═O bond being lengthened and the C(8)−C(9) and C(11)−C(12) linkages shortened relative to those in an aromatic system (Table 5). The pyridine ring exhibits characteristic shortening of its two C−N bonds. The two ring systems are not coplanar, being rotated by ca. 40° about C(4)−N(7), a geometry very similar to that observed in one of the metal complexes (**2**). The carbonyl oxygen atom forms a strong O···H−O hydrogen bond (2.583(3) Å) to the acetic acid molecule. In the crystals, the pypyd molecules form a continuous $\pi-\pi$ stack with pyridylpyridyl and pyridone-pyridone overlap, having a mean interplanar separation of 3.47 Å and a centroid-centroid distance of 3.81 Å.

Conclusions

The structural studies on the three new metal complexes reported here for pypyd show that the use of *ambidentate* extended-reach uncharged ligands provides appreciable potential

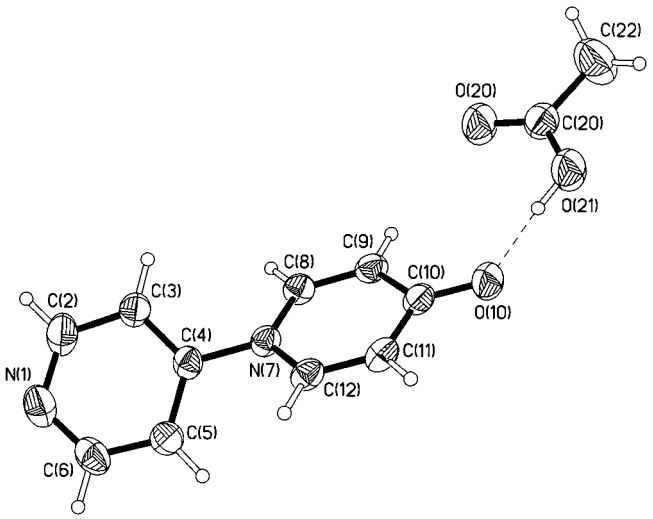

Figure 10. The molecular structure of **4** (50% ellipsoids). The O−H···O hydrogen bonding geometry is O···O, O···H 2.583(3), 1.69 Å, and the O−H···O angle is 170°.

for the generation of an extensive family of heterometallic polymeric materials, as well as further examples of homometallic arrays. Furthermore, the rigidity of this spacer ligand results in the formation of macrocycles with significant free pathways through their centers. Although not solving the frequent problem of minimization of zeotype pore-size by, for example, lattice mutual interpenetration or offset sheet interdigitation, extension of informed ligand bridge design to include those with hetero-sets of donor atoms permits the incorporation of combinations of different metal node-points as demonstrated in compounds **2** and **3**.

Clearly this approach need not be restricted to the N,O combination present in pypyd, and indeed, N,S combinations would be particularly attractive in that they would open up the possibility of synthesising a wide range of networks containing sets of both "hard" and "soft" metal ions as node points.

Acknowledgment. We thank the EPSRC for a Research Studentship (to D.A.G.) and for equipment.

Supporting Information Available: X-ray crystallographic files in CIF format for the structure determinations of $[Cu(pypyd)_2(H_2O)_2](ClO_4)_2$·pypyd **1**, $[Co_2Dy_2(pypyd)_8(H_2O)_2(NCS)_4(NO_3)_4][Co(NCS)_4]$ **2**, $[NiYb(pypyd)_4(NCS)_2(NO_3)_2]NO_3$ **3**, and pypyd·CH_3CO_2H, **4**.

IC010590H